

The Silicon Vertex Detector of the Belle II Experiment

J. Wiechczynski,^{r,*} K. Adamczyk,^r H. Aihara,^p S. Bacher,^r S. Bahinipati,^e J. Baudot,^d
P. K. Behera,^f S. Bettarini,^{j,k} T. Bilka,^b A. Bozek,^r F. Buchsteiner,^a G. Casarosa,^{j,k}
L. Corona,^k S. B. Das,^g G. Dujany,^d C. Finck,^d F. Forti,^{j,k} M. Friedl,^a A. Gabrielli,^{l,m}
B. Gobbo,^m S. Halder,ⁱ K. Hara,^{q,n} S. Hazra,ⁱ T. Higuchi,^o C. Imler,^a A. Ishikawa,^{q,n}
Y. Jin,^m M. Kaleta,^r A. B. Kaliyar,^a J. Kandra,^b K. H. Kang,^o P. Kodyš,^b T. Kohriki,^q
R. Kumar,^h K. Lalwani,^g K. Lautenbach,^c R. Leboucher,^c J. Libby,^f L. Martel,^d
L. Massaccesi,^{j,k} G. B. Mohanty,ⁱ S. Mondal,^{j,k} K. R. Nakamura,^{q,n} Z. Natkaniec,^r
Y. Onuki,^p F. Otani,^o A. Paladino,^{A,j,k} E. Paoloni,^{j,k} K. K. Rao,ⁱ I. Ripp-Baudot,^d
G. Rizzo,^{j,k} Y. Sato,^q C. Schwanda,^a J. Serrano,^c T. Shimasaki,^o J. Suzuki,^q
S. Tanaka,^{q,n} F. Tenchini,^{j,k} R. Thalmeier,^a R. Tiwary,ⁱ T. Tsuboyama,^q Y. Uematsu,^p
L. Vitale,^{l,m} Z. Wang,^p H. Yin,^a L. Zani,^{B,c} and F. Zeng^o (Belle-II SVD collaboration)

^aInstitute of High Energy Physics, Austrian Academy of Sciences, 1050 Vienna, Austria

^bFaculty of Mathematics and Physics, Charles University, 121 16 Prague, Czech Republic

^cAix Marseille Université, CNRS/IN2P3, CPPM, 13288 Marseille, France, ^Bpresently at INFN Sezione di Roma Tre, I-00185 Roma, Italy

^dIPHC, UMR 7178, Université de Strasbourg, CNRS, 67037 Strasbourg, France

^eIndian Institute of Technology Bhubaneswar, Bhubaneswar 752050, India

^fIndian Institute of Technology Madras, Chennai 600036, India

^gMalaviya National Institute of Technology Jaipur, Jaipur 302017, India

^hPunjab Agricultural University, Ludhiana 141004, India

ⁱTata Institute of Fundamental Research, Mumbai 400005, India

^jDipartimento di Fisica, Università di Pisa, I-56127 Pisa, Italy, ^Apresently at INFN Sezione di Bologna, I-40127 Bologna, Italy

^kINFN Sezione di Pisa, I-56127 Pisa, Italy

^lDipartimento di Fisica, Università di Trieste, I-34127 Trieste, Italy

^mINFN Sezione di Trieste, I-34127 Trieste, Italy

ⁿThe Graduate University for Advanced Studies (SOKENDAI), Hayama 240-0193, Japan

^oKavli Institute for the Physics and Mathematics of the Universe, University of Tokyo, Kashiwa 277-8583, Japan

^pDepartment of Physics, University of Tokyo, Tokyo 113-0033, Japan

^qHigh Energy Accelerator Research Organization (KEK), Tsukuba 305-0801, Japan

^rH. Niewodniczanski Institute of Nuclear Physics, Krakow 31-342, Poland

E-mail: wiechczynski@belle2.ifj.edu.pl

*Speaker

35 The Belle II experiment operating on the asymmetric e^+e^- SuperKEKB collider, located in Tsukuba (Japan), has been collecting data since March 2019. Its excellent vertexing abilities are provided by the vertex detector (VXD), part of which is the silicon vertex detector (SVD) that plays a crucial role in the tracking close to the interaction point. SVD operated successfully and efficiently over the whole period of data taking so far. In this article we briefly discuss its purpose, structure and basic description of the front-end electronics. The main variables related to the SVD performance are presented. The foreseen increase in SuperKEKB luminosity will lead to higher background, so we describe its impact on the SVD performance. A quick overview of the radiation campaign is presented to show the predicted behaviour of the sensors subjected to high radiation, whose level is constantly monitored. We also discuss the ongoing software development to account for the high occupancy expected in the future. In particular, the utilization of the SVD hit time information is presented as a very important quantity to suppress off-time background hits and tracks. Finally, the work done during the first long shutdown of SuperKEKB is briefly overviewed, during which a major upgrade of the pixel detector (PXD) has been successfully done. Resumption of the beam operation is expected in early 2024.

Keywords: Silicon strip detector, Vertex detector, Tracking detector, Belle II

1. Introduction

The Belle II [1] experiment is dedicated to search for physics beyond the standard model at the flavour frontier. It operates on the SuperKEKB collider located at KEK, Tsukuba in Japan, providing asymmetric beams of 7 GeV electrons and 4 GeV positrons. In the accelerator's default operation regime, the center-of-mass energy is set to the $\Upsilon(4S)$ resonance, hence it produces a huge sample of B mesons via the $e^+e^- \rightarrow \Upsilon(4S) \rightarrow B\bar{B}$ process. So far, SuperKEKB achieved the highest instantaneous luminosity of $4.7 \times 10^{34} \text{ cm}^{-2}\text{s}^{-1}$, which is the current world record. The Belle II detector is a multi-purpose spectrometer characterized by excellent vertexing capability and good hermeticity, which accumulated 424 fb^{-1} to date, and its final goal is to collect a data sample of 50 ab^{-1} , that will be possible with the constant increase of the SuperKEKB instantaneous luminosity up to our final goal of $6 \times 10^{35} \text{ cm}^{-2}\text{s}^{-1}$.

Belle II is composed of various sub-detectors with the vertex detector (VXD) closest to the beam interaction point. It divides into two further subsystems. The innermost part is the pixel detector (PXD), which is based on depleted field effect transistor (DEPFET) pixel sensors. PXD consists of two layers and its main goal is the precise determination of the decay vertices. Outside the PXD is the silicon vertex detector (SVD) [2] with four layers (numbered 3-6) that predominantly extrapolates the measured tracks to the PXD, defining so-called region of interest (ROI), which significantly reduces the amount of data recorded by PXD. SVD also performs standalone tracking for low momentum particles and contributes to the particle identification by providing energy loss (dE/dx) information.

2. SVD structure

Each layer of SVD is composed of double-sided silicon strip detectors (DSSD) that are manufactured on an n-type bulk wafer with a thickness of about $300 \mu\text{m}$ (Figure 1). One side of the bulk is covered by the p-type silicon strips placed in parallel to the beam axis that determine the $\phi - r$ coordinates (azimuthal angle and distance from the z -axis, respectively), and the n-type strips are placed perpendicularly on the other side of the bulk, measuring the z coordinate (along the beams). Figure 1 (left) shows the schematic picture of SVD layers and associated sensors with increasing numbering from the forward (FWD) to the backward (BWD) regions. Such structure is repeated along the azimuthal angle forming different ladders and the so-called windmill geometry of the SVD. The sensors differ depending on the layer and the region in which they are placed in the SVD. In the FWD part, for layers 4-6, they have a trapezoid shape and are slanted in the region that, due

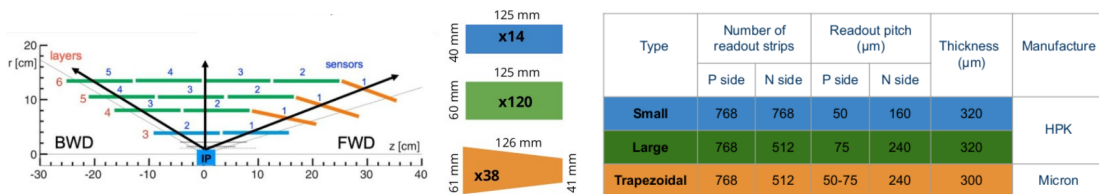


Figure 1: Schematic picture of SVD sensors forming different layers (left) and the table summarizing the parameters for each type of sensor (right).

67 to the asymmetric beams, is characterised by the highest multiplicity of the tracks. In addition, in
68 layer 3 the sensors are smaller and contain more n-type strips than the sensors in layers 4-6. This
69 also implies the readout pitch (distance between two readout strips) to be much smaller for p-side
70 strips with respect to the n-side. To improve spatial resolution, a floating strip is placed between
71 two readout strips on both p-and n-sides. The charge induced in the floating strip is shared by the
72 neighboring strips and the effective strip pitch is reduced to half of the readout pitch. The right
73 table of the Figure 1 summarises the sensor parameters. SVD consists of 224 thousand readout
74 strips and 172 sensors with an active area of 1.2 m².

75 2.1 Fornt-end electronics

76 For the readout we use APV25 chips [3]. For the central part of SVD (except for Layer 3),
77 these are attached directly to the DSSD sensors via flex circuits bent over the DSSD edge (origami
78 concept). The edge sensors use hybrid boards located outside the active volume. The APV25 has
79 128 channels per chip and amplifiers that provide a shaping time of 50 ns. Radiation hardness
80 exceeds 100 Mrad and the power consumption of the apparatus is around 0.4 W/chip. The sampling
81 frequency is 32 MHz and after the trigger's arrival we can collect six consecutive signal samples in
82 total with the multi-peak mode. To account for higher luminosity in the future, we have introduced
83 so-called "3/6 mixed acquisition mode", which allows switching between three and six samples
84 recorded on an event basis, based on the trigger type (and hence its time accuracy) for a particular
85 event. This mode, already prepared and tested, significantly reduces the data size, which can be
86 crucial in high background conditions.

87 3. SVD performance

88 Since the start of the operation we observed very smooth performance of the SVD, with very
89 few masked strips (less than 1%). Moreover, the environment has been stable and the evolution of
90 the calibration constants was consistent with expectation. Also, the effects of radiation damage are
91 well under control.

92 Several quantities related to the SVD performance - sensor efficiency, signal-to-noise ratio and
93 both spatial and time resolution - are constantly monitored. Regarding SVD sensor efficiency, the
94 values for all sensors are typically over 99% and they are also very stable over the whole period of
95 data taking. Clusters are formed from adjacent strips with significant signal and the charge collected
96 in a given cluster strongly depends on the incident angle of the track. Over time, we observe very
97 similar cluster charge in all the sensors after the normalization to the track's length. For the n-type
98 strips we observe 10-30% loss of the signal due to larger pitch. Another important variable is the
99 signal-to-noise ratio (SNR), which is satisfactory for all 172 sensors; however, a small degradation
100 is observed for the p-side due to larger noise, which is a consequence of the longer strip length
101 and hence larger inter-strip capacitance. Apart from that, we see a small deterioration of the SNR
102 with time due to radiation damage. In Figure 2 the distributions of cluster charge (left) and SNR
103 (right) are presented, where histograms representing the data accumulated in 2020 and 2022 are
104 superimposed.

105 Both position and time resolution are also very important quantities for excellent SVD perfor-
106 mance. The position resolution measurement is based on the residuals, i.e. the clusters' positions

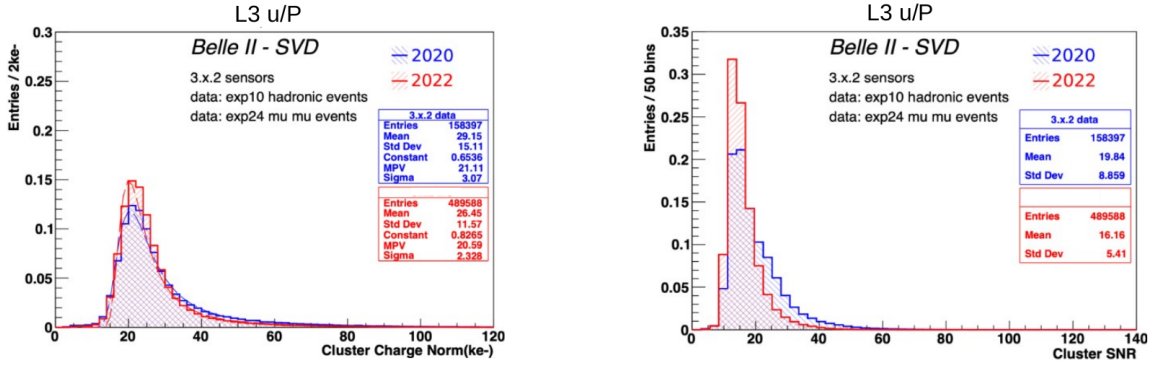


Figure 2: Distribution of Cluster Charge (left) and Signal-to-Noise Ratio (right) for Layer 3 (p-side). Comparison between data taken in 2020 (blue) and 2022 (red) is presented.

with respect to the intercept of the unbiased tracks' extrapolation, and it is evaluated with a large sample of $e^+e^- \rightarrow \mu^+\mu^-$ decays. As presented in Figure 3, this variable depends on the incident angle and is very stable during the period of the Belle II operation. As seen in Figure 3, the resolution for the n-side (left plot) is about two times worse with respect to the p-side, which is a result of different pitch.

Hit time resolution is measured with respect to the event time of the collision provided by central drift chamber (CDC) and exhibits a very good resolution of less than 3 ns for the clusters associated to tracks. Using the average value of all the hits on a given track, so called "track-time" can be computed, slightly improving the time resolution. Furthermore, the "event-time" can be determined using all the clusters associated to selected tracks in the event. In such a way, the time of the event can be computed by the SVD with resolution of the order of 1 ns, but around 2000 times faster with respect to the CDC-based computation. This feature is especially important in the higher luminosity environment, as it can significantly speed up the High Level Trigger (HLT) reconstruction process.

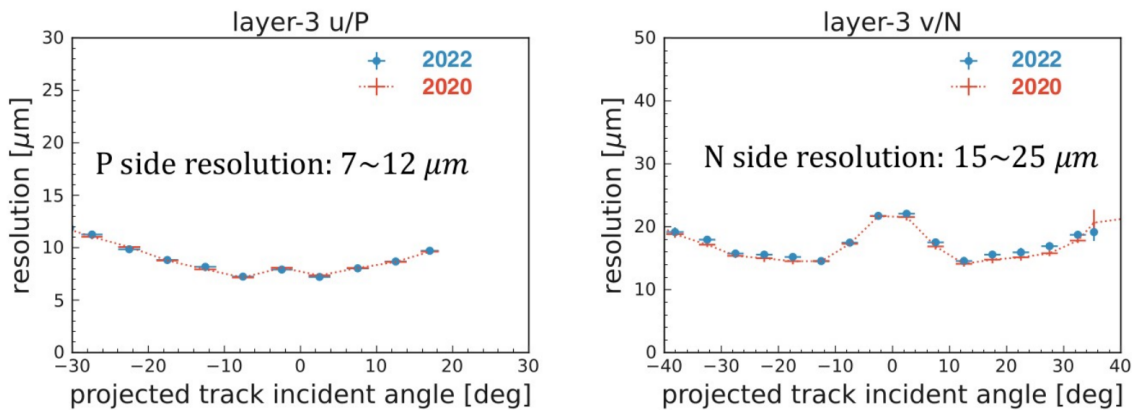


Figure 3: Distribution of position resolution for p-side (left) and n-side (right) as a function of the incident angle. Comparison between data taken in 2020 (dots) and 2022 (dotted line) is presented.

121 4. Radiation effects

122 In the high energy physics experiments, the radiation coming from the beams is a major factor
 123 that deteriorates the sensor performance with time, so the SVD dose is constantly measured by,
 124 in particular, diamond sensors. Several effects related to radiation damage must be taken into
 125 account. Firstly, the leakage current is gradually increasing and, in general, its value shows a linear
 126 dependance on the accumulated dose (Figure 4 left), that can be also expressed in the equivalent
 127 neutron fluence. So far, this increase has negligible contribution to the noise as the leakage
 128 current is still small and also due to short APV25 shaping time. This behaviour is consistent
 129 with the experience from other experiments [4] working with similar detectors and in comparable
 130 conditions. However, for the dose of ~ 6 Mrad we expect some impact on the strip noise and hence
 131 the deterioration in SNR. The strip noise itself is dominated by the inter-strip capacitance and during
 132 the operation we have observed the increase of its value for about 20% (30%) for n-side (p-side),
 133 which is expected to be saturated (Figure 4 center).

134 Another known effect of the radiation is an impact on depletion voltage. The high energy
 135 experiments usually carry out irradiation campaigns to observe the sensors' behavior after exposing
 136 them to high radiation. In the case of Belle II such a campaign has been conducted for SVD in July
 137 2022 at ELPH, Tohoku University, where the effects of high radiation up to 10 Mrad (equivalent
 138 neutron fluence: 3×10^{13} n_{eq}/cm^2) have been checked. The decrease of the depletion voltage has
 139 been observed up to the point of type inversion, which occurred at 2 Mrad ($\sim 6 \times 10^{12}$ n_{eq}/cm^2),
 140 after which the depletion voltage started to increase again (Figure 4 right). It was confirmed that
 141 the sensors will still work well after the type inversion, which meets the expectation for these types
 142 of silicon detectors. Since the beginning of the detector operation we have not observed any change
 143 of the depletion voltage and we estimate the radiation levels to be of 0.35 Mrad/year (8×10^{11}
 144 $n_{eq}/cm^2/year$) after extrapolating the background to the nominal luminosity. This ensures a wide
 145 safety margin for SVD even after 10 years of the operation at the target luminosity.

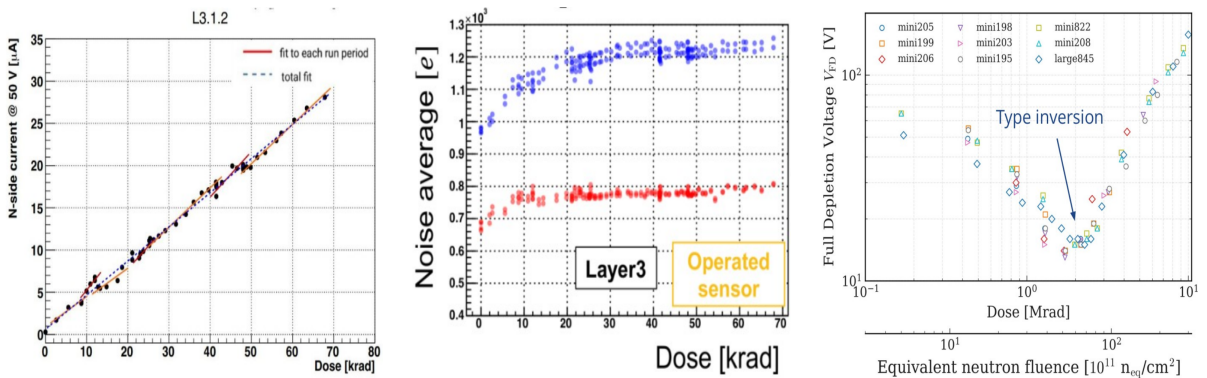


Figure 4: Left plot: Leakage current as a function of the accumulated dose; Center plot: the average noise level as a function of accumulated dose for p-side (blue dots) and n-side (red dots); Right plot: full depletion voltage as a function of the accumulated dose with the type inversion observed at 2 Mrad.

146 **5. High background scenario and related software/hardware developments**

147 An increase of the luminosity gives the effect of an increasingly larger beam background and
148 hence higher occupancy in the SVD, the direct consequence of which is the deterioration of the
149 tracking performance. So far, the average hit occupancy is 0.5% for layer 3, which does not
150 degrade the tracking. However, the background extrapolation for different future scenarios has been
151 performed based on detailed simulations of the various contributions to the background (beam-gas,
152 Toushek, etc.) and applying data/MC scale factors [5]. These studies predict that for the nominal
153 luminosity we can reach the occupancy in layer 3 very close to the limit of 4.7%, above which
154 tracking performance deteriorates. On the other hand, these predictions have large uncertainties
155 originating from poorly known machine evolution in the future, with possible redesign of the
156 interaction region. In the most conservative scenario, the layer 3 occupancy can increase up to
157 ~8.7%, which is far beyond the reasonable tracking performance. This situation motivates us to
158 develop the SVD reconstruction software, as well as consider the vertex detector upgrade [6], as
159 the safety factor might be finally too small to ensure good quality data. The technology assessment
160 related to this hardware upgrade is currently ongoing.

161 The most important effort related to the software development is the utilization of the hit time
162 information from the SVD. The real signal hits come from well-triggered collisions, but the SVD
163 acquisition window (~ 100 ns) is much wider with respect to the SuperKEKB bunch spacing (6 ns).
164 Therefore, we need to cope with many off-time hits related to the beam-induced background or
165 background from the other bunches. The current selection is based on two requirements: a) time
166 difference between p-side and n-side cluster, $|t_p - t_n| < 20$ ns, and b) cut on the absolute value of
167 the cluster time, $|t_{p,n}| < 50$ ns. These conditions reject the majority of the background hits keeping
168 above 99% of the signal, and based on them the SVD occupancy limit for layer 3 can be set at
169 4.7%. Recently, a more effective background suppression method has been developed in the form
170 of so-called “SVD grouping”. It is based on event-by-event classification of the clusters by their
171 time, so the clusters belonging to tracks from the same collisions are collected in the same group.
172 Clusters from the different collisions or beam background will be placed in the other groups, so
173 finally only the clusters belonging to the priority group will be used for the tracking. This feature
174 reduces the fake rate (fraction of the fake tracks) by 16% for the high-background scenario. An
175 additional fake rate reduction can be achieved by utilizing the selection on the track-time to reject
176 off-time tracks. Finally, these improvements allow an increase of the SVD occupancy limit for layer
177 3 from 4.7% to around 6%.

178 **6. Activities during the Long Shutdown 1**

179 Long shutdown 1 (LS1) started in May 2022 and one of the goals was to upgrade the VXD
180 detector with a new PXD. During the first data taking period, the second layer of PXD consisted
181 of two ladders only, so 5/6 of the azimuthal angle remained uncovered. The new PXD detector
182 provides the full coverage, which is beneficial for more precise vertexing. Hardware activities
183 for the VXD uninstallation and reinstallation were intense: after the VXD extraction from Belle
184 II, the SVD has been detached from the old PXD (May 16-17th, 2023), then the new PXD has
185 been attached to the SVD (20-21st June, 2023) and finally the complete VXD has been installed in

186 Belle II detector. The whole delicate procedure had no major problems or damage. In the period
187 of September 12th - October 1st, 2023, the VXD commissioning has been performed to confirm
188 the PXD and SVD performance, and also to check the impact from the increased PXD power
189 consumption and possible increase of the temperature on the sensor leak current. From September
190 21st, several cosmic runs with no magnetic field have been taken to check the performance and
191 compare them with corresponding ones for 2022 data samples. We observed no issues, in particular
192 the noise distributions over the readout channels remain basically unchanged as well as SNR for
193 the clusters associated to the tracks. Also, an excellent efficiency (>99%) for all the sensors is still
194 observed.

195 7. Conclusions

196 To conclude, SVD has successfully operated since March 2019 with very smooth performance
197 and without major problems. Its good vertexing quality has been confirmed by many physics
198 measurements, in particular those related to the lifetime analyses (e.g. Λ_c [7]). Some radiation
199 damage effects were observed, but without any impact on the performance so far.

200 However, the extrapolated background level indicates that the occupancy in the SVD can exceed
201 the current limit that guarantees good tracking performance. Hence, several software improvements
202 are being implemented to account for the high background conditions. In particular, exploitation of
203 the SVD hit time is of a major importance. Alongside, a VXD upgrade is also under discussion to
204 increase robustness against high background and matching a possible new interaction region.

205 The VXD reinstallation at Belle II with complete PXD detector has been successfully done
206 during the LS1, followed by successful VXD commissioning with cosmic data. The beam operation
207 is planned to resume in early 2024.

208 References

- 209 [1] T. Abe et al., Belle II Technical Design Report, arXiv:1011.0352 (2010).
210 [2] K. Adamczyk et al., JINST **17**, P11042 (2022).
211 [3] M. J. French et al., Nucl. Instrum. Meth. A **466**, 359 (2001).
212 [4] B. Aubert et al., Nucl. Instrum. Meth. A **729**, 615 (2013).
213 [5] A. Natchii et al., Nucl. Instrum. Meth. A **1055**, 168550 (2023).
214 [6] M. Babeluk et al., Nucl. Instrum. Meth. A **1048**, 168015 (2023).
215 [7] F. Abudinén et al., Phys. Rev. Lett. **130**, 071802 (2023)